

Viscous Film Flow in the Stagnation Region of the Jet Impinging on Planar Surface

Andrew Yeckel, Lisa Strong, and Stanley Middleman

Dept. of AMES, Chemical Engineering, University of California, San Diego, La Jolla, CA 92093

A capillary jet of liquid impinges on a planar surface that is normally oriented to the axis of the jet. The surface is initially covered with a thin uniform film of a viscous liquid. The impact and radial spreading of the liquid from the jet cause the underlying viscous film to be removed from the surface. An approximate analysis predicts the thinning rate of the film in the stagnation region of the jet. It uses the shear stress and pressure distribution of the classical Homann flow as boundary conditions for an analytical solution of the Reynolds lubrication equations in this underlying viscous film. A more exact analysis modifies the Homann flow to account for the mobility of the liquid film beneath the spreading jet and sheds light on the limitations of the analytical lubrication analysis. Data presented are in excellent agreement with the theory, subject only to the choice of a value for the hydrodynamic constant that appears in the Homann analysis.

Introduction

One of the classical problems of fluid dynamics is the axisymmetric stagnation flow, or Homann flow, in which fluid in the region $z > 0$ approaches the plane $z = 0$ with symmetry about the axis ($r = 0$) normal to the plane. The flow at infinity (that is, $z \rightarrow \infty$) is simply $U = (U_\infty, 0)$, and the solution seeks the velocity, stress, and pressure fields in the neighborhood of the surface $z = 0$. The details of the solution to this problem are given, for example, in Schlichting (1960).

We are interested in the dynamics of liquids jets that impinge on a planar surface, and in particular in the pressure and shear stress in the neighborhood of the stagnation point of the jet. Of special concern is the ability of this jet to remove, by a combination of pressure and shear forces, a very thin viscous film that initially covers the whole of the plane $z = 0$. The flow field is shown in Figure 1. This is not exactly the classical Homann flow because the jet is of a finite radius, and the ensuing flow from the jet spreads across a *mobile* viscous film, not a rigid plane. The applicability of Homann flow to the stagnation region of a jet has been argued by Chin and Tsang (1978).

In what follows, we modify and extend the classical results for Homann flow, and combine this with the Reynolds lubri-

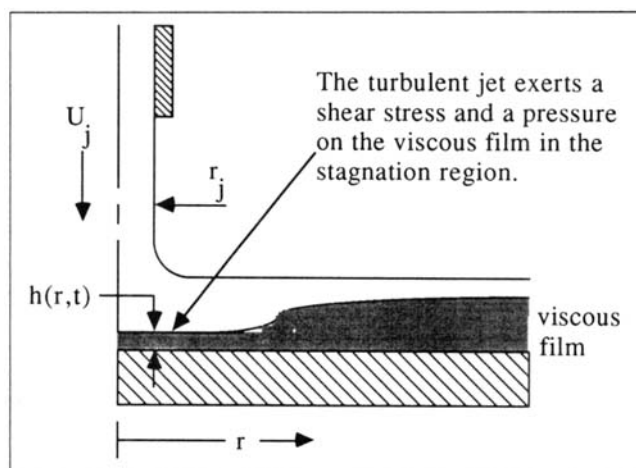


Figure 1. In the stagnation region of a turbulent jet, pressure and shear stress erode a viscous film.

cation equations for flow in the underlying thin viscous film, and obtain a prediction of the rate of thinning of the viscous film. The resulting model includes the so-called "hydrodynamic constant" for Homann flow. This "constant" is, according to Chin and Tsang, dependent on characteristics of

Present address of A. Yeckel: 2870 Holmes Ave. #301, Minneapolis, MN 55408.

Present address of L. Strong: Dept. of Chemical Engineering, University of Minnesota, Minneapolis, MN 55455.

the jet flow. We determine the constant empirically by fitting the model to data for thinning of the viscous film, and obtain a value consistent with expectations based on the discussion of this point in Chin and Tsang.

Homann Flow

The classical analysis for viscous Homann flow begins with the assumption that the velocity field may be written in the form:

$$U_r = arf'(\eta) \quad U_z = -\sqrt{2\nu a}f(\eta) \quad (1)$$

where η is defined as:

$$\eta \equiv z \sqrt{\frac{\nu}{2a}} \quad (2)$$

and a is the hydrodynamic constant. When the pressure field is written as:

$$-\frac{1}{\rho} \frac{\partial p}{\partial r} = a^2 r \quad (3)$$

the Navier-Stokes equations can be reduced to a single ordinary differential equation for $f(\eta)$ of the form:

$$f''' + ff'' + \frac{1}{2}(1 - f'^2) = 0 \quad (4)$$

with boundary conditions:

$$\begin{aligned} f = f' = 0 \quad \text{at } \eta = 0 \\ f' \rightarrow -1 \quad \text{at } \eta \rightarrow \infty \end{aligned} \quad (5)$$

The underlying viscous film is removed by the action of the jet through two mechanisms: the jet creates a radial pressure distribution in the region of the stagnation point, and the jet exerts a shear stress on the interface of the two liquids. It is necessary to have a model for these characteristics of the jet before a model for flow in the viscous layer can be developed. From the solution available for Homann flow the radial pressure distribution along the fixed plane $z=0$ is given by:

$$p(r) = \frac{1}{2} \rho U_j^2 \left[1 - \left(\frac{a^* r}{2r_j} \right)^2 \right] \quad (6)$$

where a^* is a dimensionless form of the hydrodynamic constant, defined as:

$$a^* \equiv \frac{2ar_j}{U_j} \quad (7)$$

The shear stress is given by:

$$\tau(r) = 0.656a^{*3/2} \rho U_j^2 Re_j^{-1/2} \frac{r}{r_j} \quad (8)$$

The Reynolds number is defined as:

$$Re_j = \frac{2U_j r_j}{\nu} \quad (9)$$

In all of the above, U_j is the velocity of the liquid jet at the stagnation point. The jet radius r_j appears, but always as a^*/r_j , which in fact is independent of r_j .

Approximate Analysis: Quasi-Static Film

A simple approximate analysis is possible if we assume that the underlying film is so viscous that, with respect to the flow of the jet liquid, it behaves as an immobile surface. Therefore, Eqs. 6 and 8, which apply to a jet impinging on a planar rigid surface, will be taken to apply to the case where the jet impinges on a slowly moving thin viscous film. Then these equations serve as boundary conditions on the upper surface of the viscous film. The lower boundary of the viscous film is simply the no-slip rigid surface.

If the film is thin and viscous we may neglect inertial effects, including time derivatives, in the Navier-Stokes equations for the film, and begin our analysis with the following momentum and mass balances:

$$\frac{\partial p}{\partial r} = \mu_f \frac{\partial^2 u_r}{\partial z^2} \quad (10)$$

$$\frac{\partial p}{\partial z} = 0 \quad (11)$$

and

$$\frac{\partial(ru_r)}{\partial r} + \frac{\partial(ru_z)}{\partial z} = 0 \quad (12)$$

These are essentially the Reynolds lubrication equations for a thin viscous film.

Boundary conditions take the form:

$$\mu_f \frac{\partial u_r}{\partial z} = \tau \quad \text{at } z = h(r, t) \quad (13)$$

and

$$u_r = u_z = 0 \quad \text{at } z = 0 \quad (14)$$

Equation 10 is integrated twice with respect to the z -coordinate and the solution for the velocity component u_r may be written as:

$$u_r = \frac{z}{h} \left[-\frac{h^2}{\mu_f} \frac{\partial p}{\partial r} \left(1 - \frac{z}{2h} \right) + \frac{\tau h}{\mu_f} \right] \quad (15)$$

From the continuity equation the axial velocity component is found to be:

$$u_z = -\frac{z^2}{2h^2} \left[-\frac{h^3}{\mu_f r} \frac{\partial}{\partial r} \left(r \frac{\partial p}{\partial r} \right) \left(1 - \frac{z}{3h} \right) + \frac{h^2}{\mu_f r} \frac{\partial(\tau r)}{\partial r} \right] \quad (16)$$

A kinematic condition on the film thickness connects $h(r, t)$ to the velocity components at the interface:

$$\frac{\partial h}{\partial t} + [u_r]_{z=h} \frac{\partial h}{\partial r} = [u_z]_{z=h} \quad (17)$$

After the velocity components are substituted into this kinematic condition we obtain an equation for the film thickness $h(r, t)$:

$$\frac{\partial h}{\partial t} + \left[-\frac{h^2}{2\mu_f} \frac{\partial p}{\partial r} + \frac{\tau h}{\mu_f} \right] \frac{\partial h}{\partial r} = \left[\frac{h^3}{3\mu_f r} \frac{\partial}{\partial r} \left(r \frac{\partial p}{\partial r} \right) - \frac{h^2}{2\mu_f r} \frac{\partial(r\tau)}{\partial r} \right] \quad (18)$$

with initial and boundary conditions:

$$\begin{aligned} \frac{\partial h}{\partial r} &= 0 \quad \text{at} \quad r=0 \\ h &= h_o \quad \text{at} \quad t=0 \end{aligned} \quad (19)$$

In order to solve Eq. 18 we need expressions for the pressure and shear stress distributions. In the stagnation region we have such expressions (Eqs. 6 and 8) and they are algebraically simple. As a consequence it is possible to solve Eq. 18 analytically with the result (Yeckel and Middleman, 1987):

$$\frac{1}{s} - 1 - \frac{Kh_o}{G} \ln \left(\frac{1 + \frac{Kh_o}{G} s}{1 + \frac{Kh_o}{G}} \right) = Gh_o t \quad (20)$$

where

$$\begin{aligned} s &\equiv \frac{h}{h_o} \\ K &\equiv -\frac{1}{3\mu_f r} \frac{\partial}{\partial r} \left(r \frac{\partial p}{\partial r} \right) \\ G &\equiv \frac{1}{2\mu_f r} \frac{\partial}{\partial r} (r\tau) \end{aligned} \quad (21)$$

In the stagnation region where Eqs. 6 and 8 are presumed to hold, K and G are constants, the film thickness h is independent of radial position, and:

$$\begin{aligned} \Phi &\equiv \frac{Kh_o}{G} = \frac{0.302(a^*)^2 h_o Re_j^{1/2}}{r_j} \\ \Psi &\equiv Gh_o t = \frac{0.656(a^*)^{3/2} \rho U_j^2 h_o t}{Re_j^{1/2} r_j \mu_f} \end{aligned} \quad (22)$$

This permits us to write Eq. 20 in the form:

$$\frac{1}{s} - 1 - \Phi \ln \left(\frac{1 + \Phi s}{1 + \Phi} \right) = \Psi \quad (23)$$

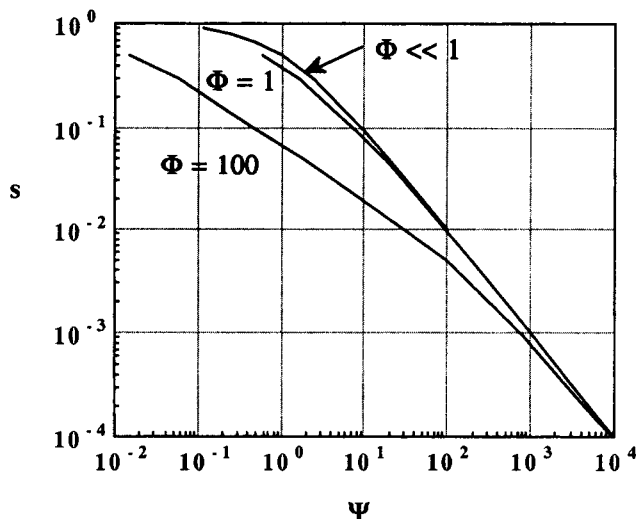


Figure 2. Film thinning in the stagnation region of a jet, according to Eq. 23.

Figure 2 shows a plot of film thickness in the stagnation region of the jet, as a function of time in this dimensionless format. We see that as s gets very small (very thin films) the model predicts that:

$$s \rightarrow \Psi^{-1} \quad (24)$$

One consequence of this asymptotic behavior is that h becomes independent of h_o at long times.

Modified Homann Flow over a Mobile Film

It is not difficult to modify the classical Homann analysis and obtain a theory for stagnation flow over a viscous but mobile film. Once this is available it is possible to determine the conditions under which the simpler theory is a good approximation to the more complete analysis. Taking note of Figure 3, we begin by rewriting Eqs. 1 and 2 for the jet flow as:

$$U_r^j = arf'(\eta_j) \quad U_z^j = -\sqrt{2\nu_j a} f(\eta_j) \quad (25)$$

where η_j is defined as:

$$\eta_j = z \sqrt{\frac{\nu_j}{2a}} \quad (26)$$

The Navier-Stokes equations for the jet still reduce to Eq. 4, but for $f(\eta_j)$:

$$f''' + ff'' + \frac{1}{2}(1 - f'^2) = 0 \quad (27)$$

and the boundary condition at infinity is:

$$f' \rightarrow 1 \quad \text{at} \quad \eta \rightarrow \infty \quad (28)$$

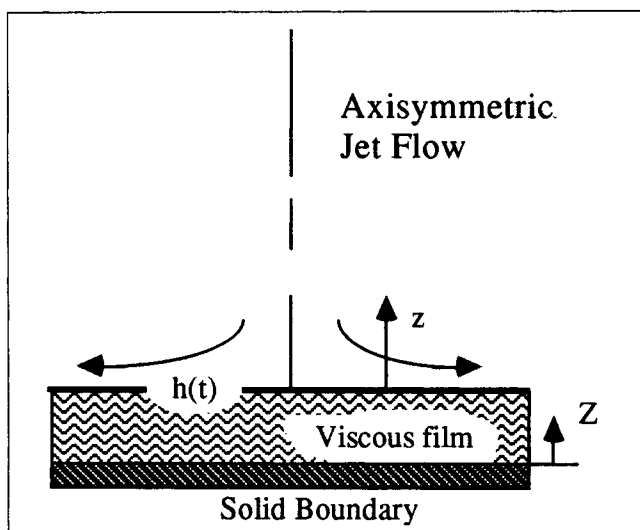


Figure 3. Geometry for the analysis of flow over a mobile film.

In the viscous liquid film ($0 < Z < h$) the velocity field is also expressed in the form:

$$U_r^f = arF'(\eta_f) \quad U_z^f = -\sqrt{2\nu_f a} F(\eta_f) \quad (29)$$

where η_f is defined as:

$$\eta_f \equiv Z \sqrt{\frac{\nu_f}{2a}} \quad (30)$$

The Navier-Stokes equations for the viscous film also reduce to Eq. 4, but for $F(\eta_f)$:

$$F''' + FF'' + \frac{1}{2}(1 - F'^2) = 0 \quad (31)$$

The no-slip condition at $Z=0$ requires that:

$$F = F' = 0 \quad \text{at} \quad \eta_f = 0 \quad (32)$$

The remaining two boundary conditions are at the interface, where the velocities and shear stresses are matched. Velocity matching requires that:

$$F' = f' \quad (33)$$

and

$$F = \sqrt{\frac{\nu_f}{\nu_j}} f = \sqrt{\frac{M}{P}} f \quad (34)$$

while the matching of the shear stresses requires that:

$$F'' = \sqrt{MP} f'' \quad (35)$$

All of these conditions are at the interface, defined by:

$$\eta_j = 0, \quad \eta_f = h/\sqrt{\nu_f/2a} \quad (36)$$

In these equations two dimensionless parameters appear:

$$M \equiv \frac{\mu_j}{\mu_f} \quad \text{and} \quad P \equiv \frac{\rho_j}{\rho_f} \quad (37)$$

It is convenient to rename the dimensionless film thickness as:

$$H \equiv h/\sqrt{\nu_f/2a} \quad (38)$$

Once a solution for F is available from the system of equations written above, the dynamics of the film thickness follow from the kinematic condition:

$$\frac{dh}{dt} = U_z^f(h) = -\sqrt{2\nu_f a} F(H) \quad (39)$$

or

$$\int_H^{H_0} \frac{d\eta_f}{F} = T \equiv 2at \quad (40)$$

To evaluate the validity of the approximate lubrication analysis presented earlier (Eq. 23) we first note that Φ and Ψ of that analysis may be written as:

$$\Phi = 0.359 H_0 M^{-1/2} \quad \text{and} \quad \Psi = 0.464 P H_0 M^{1/2} T \quad (41)$$

Thus, we will examine the behavior of s vs. Ψ , where now we can write Ψ as:

$$\Psi = 0.464 P H_0 M^{1/2} \int_H^{H_0} \frac{d\eta_f}{F} \quad (42)$$

Solutions for Flows in Two Fluids, and Evaluation of Limitations of Quasi-Static Approximation

Equations 27 and 31 are a coupled set of third-order ordinary differential equations with the coupling arising through the matching conditions at the interface between the two fluids. The equations are integrated numerically. Because there are some convergence problems that arise in the solution procedure, we offer a few brief comments regarding a successful method of solution. The two equations are rewritten as six first-order equations, and they are integrated using a fourth-order Runge-Kutta method. A shooting method is used to recast the boundary-value problem as an initial-value problem. The equations for F are integrated from the wall to the interface, at which point the matching conditions are applied. Then the equations for f are integrated to "infinity," which is taken to be ten dimensionless units (in h_j) from the interface.

To begin the integration it is necessary to provide an initial estimate of the value of F'' at the wall. This estimate is refined until the limiting value of f' far from the wall satisfies the boundary condition there. The problem of refining the estimate of F'' is that of solving one nonlinear equation for a single unknown. Newton's method was used for this purpose.

Newton's method will not converge if the initial estimate of F'' is too far from the true value. Because of this it is always

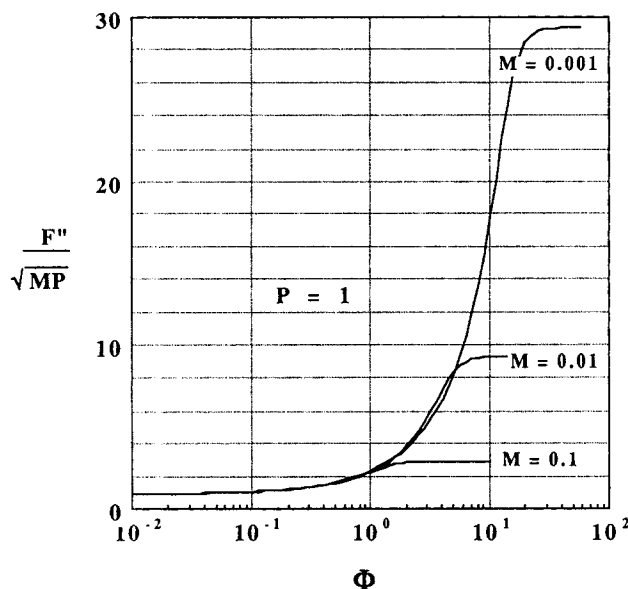


Figure 4. Dimensionless wall shear stress (F''/\sqrt{MP}).

wise to combine Newton's method with a continuation scheme, whereby a known value of F'' at one set of parameters is used as an initial estimate to solve the problem at a nearby set of parameters. A logical starting point is the limiting case of infinitesimal film thickness, for which the value of F'' is known from the classical Homann analysis. After the first solution is obtained, the problem is solved repeatedly for progressively thicker films, using the value of F'' from the most recent case as the initial guess for the next case.

Once F is known, it is a simple matter to integrate the dynamic equation for the film thickness (Eq. 40) as a function of time. The trapezoid rule proves adequate for this purpose.

Figure 4 shows a plot of the shear stress at the wall as a function of the film thickness Φ , defined in Eq. 41. The dimensionless shear stress is expressed as F''/\sqrt{MP} . Note in particular that the *jet* viscosity is used in this nondimensionalization. Figure 5 shows the same thing for the shear stress at the jet-film interface, expressed as f'' . In both plots curves are shown at three values of the viscosity ratio M . The density ratio is set at the value $P=1$ in all cases to reflect our interest in liquid-liquid systems. In both figures the stress approaches the value obtained from the Homann analysis ($f''=0.929$) as Φ tends toward zero, an expected result.

The approximate analysis given earlier is based on the assumption that the shear stress at the interface of the two liquids is virtually identical to the Homann value for a single fluid. If the film is sufficiently thin and viscous that the decrease in shear stress from the interface to the wall is small, relative to the Homann value, we expect that this approximation will be a good one. A comparison of Figures 4 and 5 shows that this is the case at values of Φ up to about 0.1. A fortuitous result (Figure 5) is that the interface stress remains close to the Homann value at values of Φ an order of magnitude greater, up to $\Phi=1$, at which point the wall stress is more than twice the Homann value.

Another result to consider is that the approximate model leads to the prediction that the nondimensional shear stress

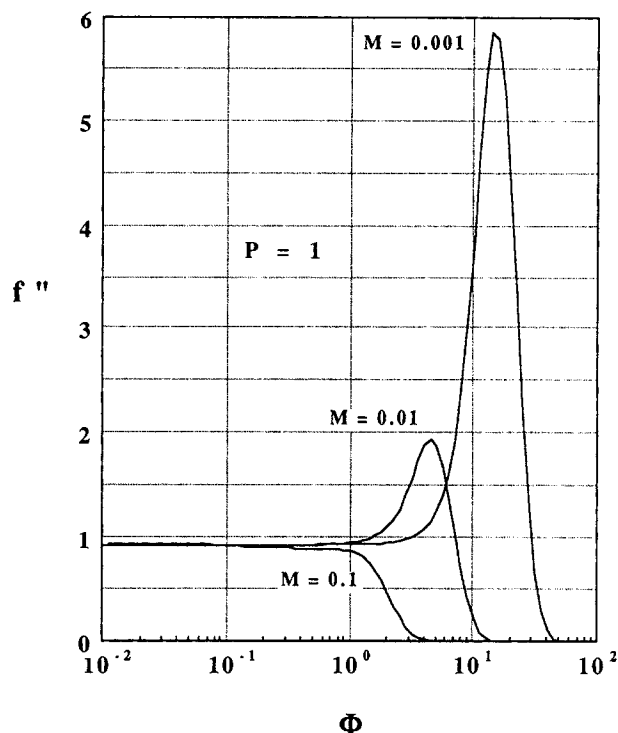


Figure 5. Dimensionless interface shear stress (f'').

depends only upon Φ , whereas in the more general model additional parameters M and P appear. Figures 4 and 5 (for a fixed value of $P=1$) show that the dimensionless wall and interface stresses are independent of M up to values of Φ of about unity, the same point at which the interface stress begins to diverge from the Homann value.

Figure 5 shows that for Φ greater than one, the interface stress diverges sharply from the Homann value, in which case clearly the approximate model fails. At large enough Φ the interface stress falls to zero. That the interface stress has fallen to zero indicates that viscous effects are confined to the film, and the jet consists of a potential flow right up to the interface. Under these conditions, only the force caused by the radial pressure gradient acts to remove the viscous film. From this point on, the dimensionless *wall* stress is a constant, equal to the Homann stress (based on the jet viscosity) divided by the square root of M , as seen in the large Φ asymptotes of Figure 4. If the wall stress is made dimensionless by the *film* viscosity rather than the jet viscosity, the dimensionless wall stress equals the Homann value. This indicates that the jet transfers its momentum without viscous loss to the film, which itself is in a state of Homann flow.

The use of the shear stress at the solid boundary according to the *single-fluid* Homann analysis, as an approximation to the shear stress at the mobile interface in the two-fluid case, is seen to be a good approximation if the initial film thickness is so small that $\Phi < 0.03$. Under these conditions we would expect that the simple analytical lubrication analysis will be an accurate model of flow in the viscous film. It turns out that the approximate lubrication model for the dynamics of the film thinning is accurate to even higher values of Φ , as Figure 6 shows.

In Figure 6 we see a comparison of the approximate lubri-

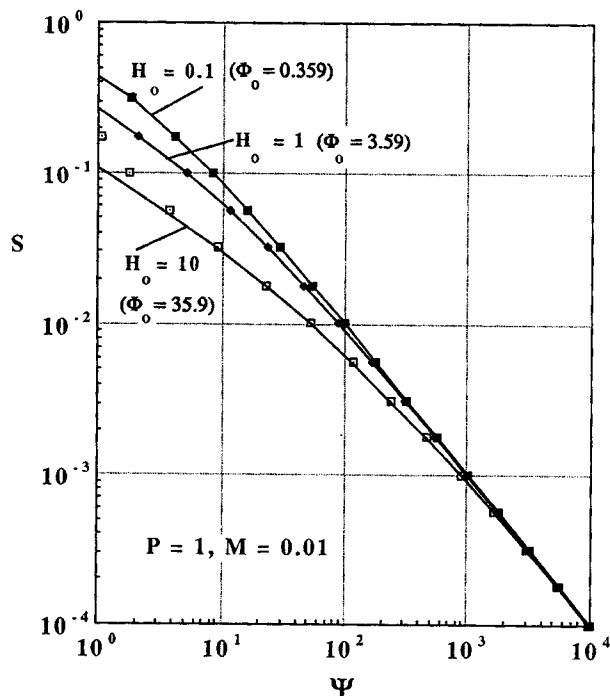


Figure 6. Comparison of the simple approximate (lubrication) model to the exact (two-fluid Homann) analysis for the rate of thinning of the mobile film.

Symbols are exact solution—lines are lubrication theory.

cation analysis (the solid curves) and the mobile-film two-fluid Homann analysis for the rate of thinning of the mobile film. Results are shown for selected values of the parameters P and M . With these choices, selection of an H_o value fixes the value of Φ_o , at the values shown. The approximate model coincides nearly perfectly with the more exact model, even for short times (small Ψ) where the film is relatively thick, when H_o is smaller than unity. For the relatively large value of $H_o = 10$ ($\Phi_o = 35.9$) we see a significant deviation of the two models of the film thickness history at short times. However, as the initially thick film grows thinner, the behavior of s vs. Ψ becomes independent of h_o , the two models coincide, and both models exhibit the expected approach of s to $1/\Psi$.

Experimental Studies

We have carried out some experimental tests of the ability of Eq. 23 to mimic observations on film thinning under an impinging turbulent jet of water. The experiments were designed to produce very thin (submicron) viscous films on an extremely smooth planar surface. Thin films of silicone oil (polydimethylsiloxane) were spin coated onto electronic grade silicon wafers. Turbulent jets of water were used to "remove" the film, and the residual film thickness at the stagnation point of the jet was measured as a function of time. Film thickness was measured directly on the wafer using an optical method based on ellipsometry. A Rudolph Research Auto E1 II auto-nulling ellipsometer was used. All experiments were carried out inside a Modulair MS-100 laminar flow hood in order to reduce the risk of particle contamination of these thin films. A more complete discussion of some of the issues associated

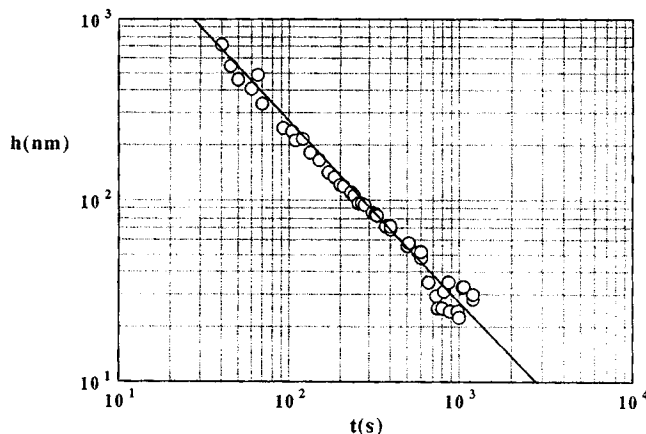


Figure 7. Thinning of a film of silicone oil in the stagnation region of a turbulent water jet.

The silicone oil has a kinematic viscosity of 1,000 centistokes; the jet issues from a capillary of inside diameter $D = 4.57$ mm at a volume flow rate of $68 \text{ cm}^3/\text{s}$. The Reynolds number of the jet (based on capillary diameter) is 19,000.

with accurate film thickness measurements of this type can be found in Strong and Middleman (1989).

In order for Eq. 23 to yield a predictive model for $h(t)$ it is necessary to have a value for the dimensionless hydrodynamic constant a^* . Experimental data cited by Chin and Tsang suggest that a^* is of order unity, but it depends to some degree on the ratio of the capillary radius to the distance the jet travels from the capillary exit to the horizontal plane.

Nakoryakov et al. (1978) have made extensive measurements of the wall stress under an impinging jet, and they find that over a range of jet Reynolds numbers from 17,000 to 41,000, a single value of $a^* = 0.88$ permits their data to be fit very well by the single-fluid Homann analysis.

An example of our data on film thinning (at a jet Reynolds number of 19,000) is shown in Figure 7. With $a^* = 0.88$, Eq. 23 yields the line shown. The data are very well described by the approximate two-fluid model. We note that in the range of 20 to 40 nm film thickness the scatter in the measurements increases. We believe this is due to optical effects arising from silicon surface roughness of the order of 2 nm. This latter measurement follows from a series of studies of the surfaces of the bare silicon wafers, using a Sloan Dektac 3030 Surface Profilometer.

Discussion and Conclusions

The classical Homann flow analysis can be used to supply boundary conditions for the Reynolds lubrication equations for flow within a thin viscous film, leading to a model for the thinning of the film in the stagnation region of a turbulent water jet. The model involves a single arbitrary parameter, the so-called "hydrodynamic constant" of Homann flow. Over a range of evolving film thicknesses, from 1,000 down to about 40 nm, the data are very well described by this model. In this approximate model it is assumed that the underlying liquid film moves slowly with respect to the jet flow and experiences the same shear stress at the upper (mobile) surface that it would if the underlying film were stationary.

A more exact theory which relaxes the simplifying assumption about the shear stress at the mobile surface is developed.

The lubrication approximation is dropped, and the equations for the flows in the underlying viscous film and in the jet flow are solved instead using the approach of Homann. The results are compared to those of the approximate lubrication theory. Conditions under which there is a significant deviation of the two models are indicated.

A key assumption of the models displayed here is that the mobile interface is stable. It is well-known that parallel flows of this type have the capacity to display several modes of instabilities. (See, for example, the works of Joseph et al., 1984, Papageorgiou et al., 1990, and Preziosi et al., 1989). No such instabilities have been observed in our experimental studies reported here, and we have not pursued this particular line of inquiry.

Literature Cited

Chin, D.-T., and C.-H. Tsang, "Mass Transfer to an Impinging Jet Electrode," *J. Electrochem. Soc.*, **125**, 1461 (1978).

Joseph, D., M. Renardy, and Y. Renardy, "Instability of the Flow of Two Immiscible Liquids with Different Viscosities in a Pipe," *J. Fluid Mech.*, **141**, 309 (1984).

Nakaryakov, V. E., B. G. Pokusaev, and E. N. Troyan, "Impingement of an Axisymmetric Liquid Jet on a Barrier," *Int. J. Heat Mass Transfer*, **21**, 1175 (1978).

Papageorgiou, D. T., C. Maldarelli, and D. S. Rumschitzki, "Non-linear Interfacial Stability of Core-annular Film Flows," *Phys. Fluids A*, **2**, 340 (1990).

Preziosi, L., K. Chen, and D. Joseph, "Lubricated Pipelining: Stability of Core-Annular Flow," *J. Fluid Mech.*, **201**, 323 (1989).

Schlichting, H., *Boundary Layer Theory*, McGraw-Hill, New York, p. 81 (1960).

Strong, L., and S. Middleman, "Lubricant Retention on a Spinning Disk," *AIChE J.*, **35**, 1753 (1989).

Yeckel, A., and S. Middleman, "Removal of a Viscous Film from a Rigid Plane Surface by an Impinging Liquid Jet," *Chem. Eng. Commun.*, **50**, 165 (1987).

Manuscript received Aug. 11, 1993, and revision received Nov. 22, 1993.